Arch Appl Mech (2020) 90:1705–1722
https://doi.org/10.1007/s00419-020-01691-6

ORIGINAL

Shun Hu Zhang · Xing Rui Jiang · Chong Chen Xiang · Lei Deng · Yin Xue Li

Proposal and application of a new yield criterion for metal plastic deformation

Received: 14 October 2019 / Accepted: 28 February 2020 / Published online: 11 March 2020

Abstract A new linear yield criterion in terms of principal stresses is developed for the purpose of overcoming the analytical difficulty of mechanical parameters when using the nonlinear Mises yield criterion. This developed yield criterion is established through the parabola interpolation method and the mathematical averaging method, which can be called as the mean influence factor yield criterion, or called MIF yield criterion for short. The yield locus of the criterion on the π-plane is an equilateral and non-equiangular dodecagon, lies between the Tresca and TSS loci, and is very close to the locus of the Mises yield criterion. By comparing with the classical yield criteria, the MIF yield criterion varies linearly with the Lode parameter and has a good accuracy with experimental data. Moreover, based on the flow rule and the geometric projection of the principle stress components, the specific plastic work rate of the yield criterion is also derived. The criterion and its specific plastic work rate are used to solve the limit load of a simply supported circular plate and the forging of a rectangular bar, and both the corresponding analytical solutions are obtained. The theoretical results for the limit load and the forging force are in good agreement with the simulation and experimental data, respectively, and are more accurate than the results calculated from other yield criteria.

Keywords Yield criterion · Plastic deformation · Limit load · Forging force · Analytical solution

1 Introduction

The development and utilization of material strength is a basic and important research content in the field of metal deformation. With the research progress on the plastic forming process, the basic criterion for describing material deformation has been paid more and more attention. At present, there are more than a few dozen kinds of yield criteria proposed by many researchers.

For the yield criterion, the earliest mechanical research result was proposed by Coulomb [1] in 1776, which is usually called the maximum strength theory. This theory assumes that if the plane shear stress exceeds the resultant stress caused by the cohesive force and friction force, the material will deform in the form of sliding. On the basis of blanking and extrusion experiments in 1864, the maximum shear stress theory was put forward by Tresca [2]. He assumed that a metal will yield as long as the maximum shear stress reaches a limit value. The calculation based on this criterion is relatively simple, but only the maximum principal shear stress is considered. Thus, the Tresca yield criterion belongs to the single shear stress yield criterion. Based on this yield

S. H. Zhang · X. R. Jiang · C. C. Xiang (✉) · L. Deng · Y. X. Li
Shagang School of Iron and Steel, Soochow University, Suzhou 215021, China
E-mail: ccxiang@suda.edu.cn

S. H. Zhang
State Key Laboratory of Materials Processing and Die & Mould Technology, Huazhong University of Science and Technology, Wuhan 430074, China

criterion, Saint-Venant [3] and Levy [4] have made further researches in rigid plastic theory. They pointed out that the principal axes of plastic strain rate are the same as that of stress during metal forming process.

In 1913, von Mises proposed a new yield criterion that was originally proposed by Huber in 1904 [5,6]. He considered a general yield condition that as long as the second deviatoric stress invariant reaches a certain value, then the metal will transform from elastic deformation to plastic deformation. The influence of the intermediate principal stress is also considered in the Mises yield criterion. After Hencky and Nadai's [7] experiments, it is known that the Mises yield criterion can conform better to the experimental data. However, the expression of the Mises criterion is nonlinear and does not consider the hydrostatic pressure. Later, von Mises [8] formulated the Hill criterion in 1928 and demonstrated that at least five independent strain components are needed for plastic deformation of a constant volume solid. For the research convenience, Hill [9] established a basic framework for the classical theory of yield criteria, and extended the Mises criterion to his own yield criterion. In 1951, Drucker and Prager [10,11] put forward a basic assumption about yield surface. It is considered that when the material is yielding, the octahedral shear stress is linearly dependent on the octahedral normal stress. By adding the hydrostatic pressure into the Mises formula, Drucker obtained a nonlinear yield criterion for soils exhibiting the dilatancy during plastic flow, which has less usage in analytical investigation of metal forming due to its complexity of the expression. Haigh and Westgaard [12] unified the forms of various criteria in the three-dimensional principle stress space, and then proposed the conception of setting $\sigma_1, \sigma_2, \sigma_3$ as the principal axes to form the 3-D stress space. Each point in the space represents a stress state, and the yield surface can be expressed by a curve in the stress space.

In recent decades, there have been great achievements in the study of yield criteria. In 1983, Yu [13,14] put forward the TSS yield criterion. He assumed that a material will yield when the combination of the two larger principal shear stresses attains a critic value. The yield locus of the TSS yield criterion is a hexagon which circumscribes the Mises circle on the yield plane. The loci of other yield criteria, such as Tresca and Mises yield criteria, usually won't exceed the TSS yield criterion, that is, the TSS yield criterion provides the upper bound of the results. Later, Yu [15] proposed the UYC yield criterion, whose expression is composed of two maximal principal shear stresses with different weighting coefficients, and the yield curve is discontinuous. In 2005, Yu et al. [16] considered that although the twin shear stress yield criterion considered the influence of the intermediate principal stress, the influence of the minimum shear stress on material strength is still not taken into account. Therefore, a three-shear stress yield criterion was also proposed. In the analysis of plastic failure of pipeline, a yield criterion called ASSY was proposed by Zhu et al. [17,18]. This criterion is the average of the Tresca and the Mises yield criterion and is also a nonlinear function. It has been applied successfully in predicting the failure pressure of pipeline. In order to explain the yield conditions of ductile and brittle materials, Barsanescu et al. [19] proposed a modified Mises yield criterion by introducing a modified coefficient in terms of the maximum strain energy and maximum distortion energy. For homogeneous isotropic materials, Gu et al. [20] proposed two failure formulas for two different cases of tension and compression. He assumed that shape distortion and volume dilation would lead to material failure, while volume contraction, such as hydrostatic compression, would impede the failure. Pei et al. [21] introduced a normal stress space consisting of three normal stresses in the material coordinate system to express the interaction between stress tensor and material structure. Then, the anisotropic Matsuoka–Nakai (AMN) criterion is proposed to describe the anisotropic shear strength of rock based on geometric factors rather than algebraic tensors. Böhlke et al. [22] analyzed the correlation of the elastic and plastic anisotropy with experimental and theoretical method and developed a phenomenological model which can estimate the plastic anisotropy of the polycrystal. Recently, based on dislocation theory, several modern physical models that capable of predicting work hardening have been initiated by Langer et al. [23,24] and further devolved by Le et al. [25,26].

On the basis of predecessors' researches, it can be seen that: The Tresca yield criterion usually gives the lower bound solution, and the TSS yield criterion usually gives the upper bound solution; the predictive precision of the Mises yield criterion is high but its formula is nonlinear, which is very hard to be used in obtaining the analytical solution of mechanical parameters. So, it is desire to seek a high precise yield function whose expression has linear characteristic and can close well to the Mises yield criterion.

Based on this idea, this paper attempts to obtain the characteristic points of the influence factor of the intermediate principal stress from the expressions of the three yield criteria, i.e., the Tresca, Mises, TSS yield criteria, and to establish a parabolic function through the calculated characteristic points. The present characteristic point is obtained through the parabolic interpolation method and the mathematical averaging method and a new linear yield criterion in terms of principal stresses is developed. The calculation solution with the proposed yield criterion is verified by the experimental data, and a good agreement is found. The yield

criterion and the derived specific plastic work rate are also applied to the calculation of the limit load and the forging analysis of rectangular bar, respectively, and the corresponding analytical solutions are obtained.

2 Derivation of the MIF yield criterion

2.1 Mathematical derivation

In 1864, Tresca has made a famous assumption that yielding occurs when the maximum shear stress of a material reaches its limit [2]. According to his assumption, the following expression to describe the yielding of a material can be written as

$$f^{\text{Tresca}} = \sigma_1 - \sigma_3 - \sigma_s = 0 \tag{1}$$

where σ_1 is the first principle stress, σ_3 is the third principle stress, σ_s is the yield strength of a material.

The Mises yield criterion was proposed by von Mises [3] in 1913, which suggests that yielding of a materiel occurs if the invariant of the second deviatoric stress reaches a critical value. Mathematically, the Mises yield criterion can be expressed as

$$f^{\text{Mises}} = (\sigma_1 - \sigma_2)^2 + (\sigma_2 - \sigma_3)^2 + (\sigma_3 - \sigma_1)^2 - 2\sigma_s^2 \tag{2}$$

where σ_2 is the intermediate principle stress.

Equation shows (2) that the Mises yield criterion is a nonlinear function of $\sigma_1, \sigma_2, \sigma_3$, which is difficult to be used in obtaining analytical solutions of mechanical parameters, although it will not cause any problems from a numerical point of view. As given, a linearization of this criterion is still worthwhile.

The twin shear stress (TSS) yield criterion was developed by Yu [13] in 1983. It suggests that yielding occurs if the combination of the two larger principal shear stresses satisfies the following relation:

$$f^{\text{TSS}} = \sigma_1 - \frac{1}{2}(\sigma_2 + \sigma_3) - \sigma_s = 0, \quad \sigma_2 \le \frac{1}{2}(\sigma_1 + \sigma_3) \tag{3a}$$

$$f^{\text{TSS}} = \frac{1}{2}(\sigma_1 + \sigma_2) - \sigma_3 - \sigma_s = 0, \quad \sigma_2 \ge \frac{1}{2}(\sigma_1 + \sigma_3). \tag{3b}$$

The yield loci of the above criteria are shown in Fig. 1. In this figure, the Mises locus is a circle, the Tresca locus is an inscribed regular hexagon of the Mises circle, and the TSS locus is a circumscribed regular

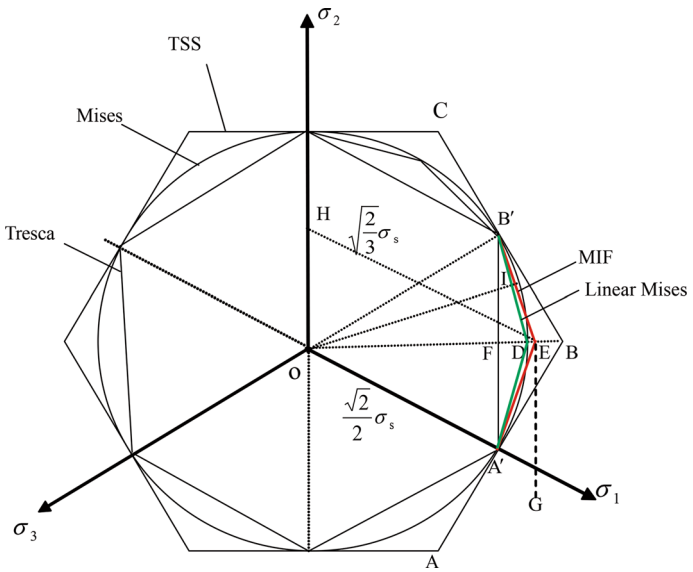

Fig. 1 Different yield loci on the π-plane

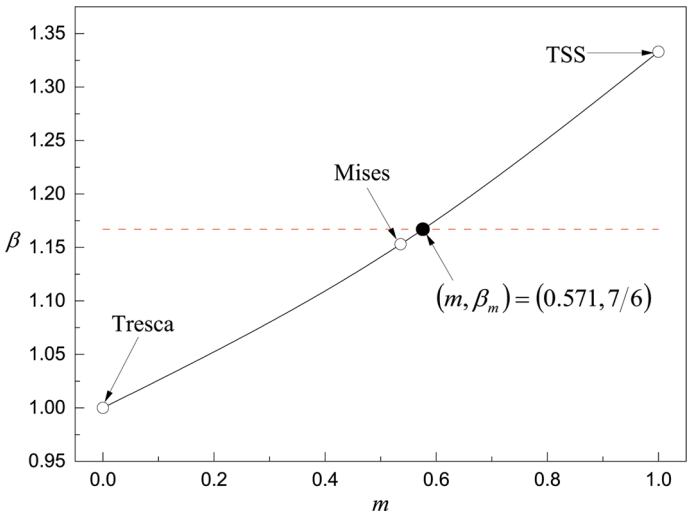

Fig. 2 The curve of parabolic equation

hexagon of the Mises circle. It is seen that the points F, D, and B are on the Tresca, Mises, and TSS yield loci, respectively.

The above three yield criteria can be generalized to the following linear form:

$$\begin{aligned} &\sigma_1 - \frac{m}{2}\sigma_2 - \left(1 - \frac{m}{2}\right)\sigma_3 = \sigma_s, \quad \sigma_2 \le \frac{1}{2}(\sigma_1 + \sigma_3) \\ &\left(1 - \frac{m}{2}\right)\sigma_1 + \frac{m}{2}\sigma_2 - \sigma_3 = \sigma_s, \quad \sigma_2 \ge \frac{1}{2}(\sigma_1 + \sigma_3) \end{aligned} \tag{4}$$

where the criterion with $m = 0$ refers to the Tresca yield criterion, the criterion with $m = 2(2 - \sqrt{3})$ refers to the approximated Mises yield criterion in a linear form [14], and the criterion with $m = 1$ refers to the TSS yield criterion.

In order to evaluate the influence of the intermediate principal stress on yielding, Eq. (4) is rewritten as

$$\sigma_1 - \sigma_3 = \beta\sigma_s \tag{5}$$

where $\beta = 2/\sqrt{3 + \mu_d^2}$ is the influence factor of the intermediate principal stress, and μ_d is the Lode parameters, written as [27]

$$\mu_d = \frac{\sigma_2 - \frac{\sigma_1 + \sigma_3}{2}}{\frac{\sigma_1 - \sigma_3}{2}} \tag{6}$$

The intermediate principal stress $\sigma_2 = [\sigma_1 + \sigma_3 + \mu_d(\sigma_1 - \sigma_3)]/2$ can be substituted into the above yield criteria, then the β can be calculated. The case with $\beta = 1$ corresponds to the Tresca criterion, $\beta = 2/\sqrt{3}$ corresponds to the Mises criterion, and $\beta = 4/3$ corresponds to the TSS criterion.

From the above correspondence between m and β, we can construct a parabolic equation through these three points, i.e., $(0,\ 1)$, $(4 - 2\sqrt{3}, 2/\sqrt{3})$, $(1,\ 4/3)$, which can be expressed as

$$\beta = \frac{2}{\sqrt{3 + \mu_d^2}} = \frac{\sqrt{3}}{18}m^2 + \frac{6 - \sqrt{3}}{18}m + 1 \tag{7}$$

Equation (7) shows that the Lode parameter is related to the m. Based on Eq. (7), the corresponding parabolic curve, β versus m, is illustrated in Fig. 2.

In this figure, β_m is the mean value of the β^{Tresca} and β^{TSS}, i.e., $\beta_m = (\beta^{\text{Tresca}} + \beta^{\text{TSS}})/2 = 7/6$, which is calculated here to derive a new yield criterion that can lies in between the Tresca and the TSS yield criteria. Substituting it into the parabolic equation, the value of m can be solved out as $(1 - 2\sqrt{3} + \sqrt{13})/2$.

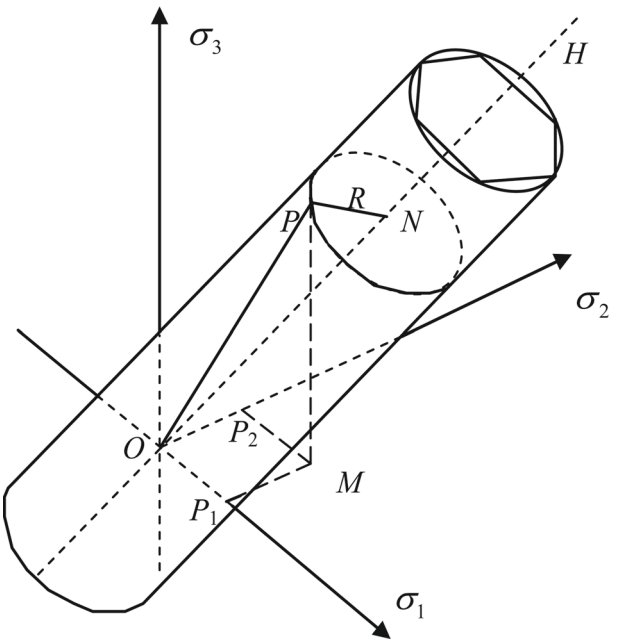

Fig. 3 The yield locus of the Mises criterion

Therefore, the new yield criterion can be called as the mean influence factor yield criterion, abbreviated as MIF yield criterion.

Thus, the yield function of the MIF yield criterion in terms of principal stresses can be expressed as

$$f_{A'E}^{\mathrm{MIF}} = \sigma_1 - \frac{1-2\sqrt{3}+\sqrt{13}}{4}\sigma_2 - \frac{3+2\sqrt{3}-\sqrt{13}}{4}\sigma_3 = \sigma_s, \quad \sigma_2 \le \frac{\sigma_1+\sigma_3}{2} \tag{8a}$$

or

$$f_{B'E}^{\mathrm{MIF}} = \frac{3+2\sqrt{3}-\sqrt{13}}{4}\sigma_1 + \frac{1-2\sqrt{3}+\sqrt{13}}{4}\sigma_2 - \sigma_3 = \sigma_s, \quad \sigma_2 \ge \frac{\sigma_1+\sigma_3}{2} \tag{8b}$$

The equation shows that the yielding of a materiel occurs when the linear combination of the stress components $\sigma_1, \sigma_2, \sigma_3$ is in accordance with the coefficient of $1, -(1-2\sqrt{3}+\sqrt{13})/4, -(3+2\sqrt{3}-\sqrt{13})/4$ or $(3+2\sqrt{3}-\sqrt{13})/4$, $(1-2\sqrt{3}+\sqrt{13})/4$, -1. Compared with the Mises yield criterion, it can be seen that the proposed yield criterion can provide the calculation advantage due to its linearity. However, it should be noted that since the new yield criterion is a piecewise function and its yield locus at each intersected point, such as the point E in Fig. 1, is discontinuous. This indicates that its differentiable ability is not as good as that of the Mises yield criterion. Before using this new yield criterion, it is necessary to analyze the stressed characteristics of a specific structure, i.e., $\sigma_2 \ge (\sigma_1+\sigma_3)/2$ or $\sigma_2 \le (\sigma_1+\sigma_3)/2$, and then to determine which piecewise function is suitable.

2.2 Yield locus of the MIF yield criterion

In the principal stress space, the vector $\overrightarrow{OP}$, as shown in Fig. 3, is a resultant vector which is combined of the vector components $\overrightarrow{OP}_1$, $\overrightarrow{OP}_2$, and $\overrightarrow{MP}$.

By geometrical projection, it can be seen that the point P corresponds to the point D on the π-plane. From Figs. 1 and 2, the projection of the OD on the π-plane can be calculated as:

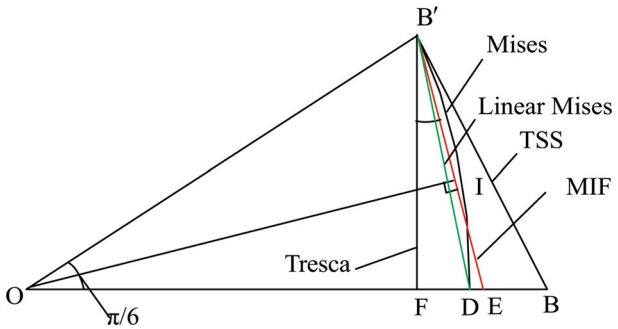

Fig. 4 The yield locus of MIF criterion on the π-plane

$$OG = OB = \sqrt{\frac{2}{3}}\sigma_1 = \frac{1}{\cos 30^\circ} \cdot \sqrt{\frac{2}{3}}\sigma_s = \frac{2\sqrt{2}}{3}\sigma_s \tag{9}$$

$$\sigma_1 = \tfrac{2}{\sqrt{3}}\sigma_3,\ \ \sigma_3 = 0,\ \ \sigma_2 = \frac{\sigma_1 + \sigma_3}{2} \tag{10}$$

$$OH = GD = \sqrt{\frac{2}{3}}\sigma_2 = \frac{2\sqrt{2}}{3}\sigma_s \cdot \sin 30^\circ = \frac{\sqrt{2}}{3}\sigma_s,\ \ \sigma_2 = \frac{\sigma_s}{\sqrt{3}} \tag{11}$$

Substituting $\sigma_1, \sigma_2, \sigma_3$ into the Mises yield criterion function, then we can have

$$f_D^{\text{Mises}} = \frac{1}{\sqrt{2}}\sqrt{\left(\frac{2}{\sqrt{3}}\sigma_s - \frac{\sigma_s}{\sqrt{3}}\right)^2 + \left(\frac{\sigma_s}{\sqrt{3}}\right)^2 + \left(-\frac{2}{\sqrt{3}}\sigma_s\right)^2} = \sigma_s \tag{12}$$

The result in Eq. (12) means that yielding of the material with the stress state at the point D occurs. Substituting σ_1, σ_2, and σ_3 into the MIF yield criterion, it produces

$$f_D^{\text{MIF}} = \frac{2}{\sqrt{3}}\sigma_s - \frac{1 - 2\sqrt{3} + \sqrt{13}}{4} \cdot \frac{1}{\sqrt{3}}\sigma_s = 0.989578\sigma_s \tag{13}$$

The coefficient of σ_s in Eq. (13) is smaller than 1, which means that this stress state at E has not yielded according to the MIF yield criterion. Thus, the yield point E must be outside of D. The distance between E and D is determined by the difference between the two formulas on the π-plane. Therefore, the length of ED can be calculated

$$ED = \sqrt{\frac{2}{3}}\left(f_D^{\text{MIF}} - f_D^{\text{Mises}}\right) = 0.0085095\sigma_s \tag{14}$$

That is to say, the location of point E is $0.0085095\sigma_s$ outside of D. By connecting $A'E$, $B'E$, we can get the locus of the MIF criterion, which is illustrated in Fig. 4.

The length of the side of the dodecagon and the apex angle are calculated as follows:

$$\begin{cases} \tan\angle FB'E = \left(\sqrt{\frac{2}{3}}\sigma_s - \frac{\sqrt{2}}{2}\sigma_s + ED\right) \Big/ \frac{1}{2}\sqrt{\frac{2}{3}}\sigma_s = 0.2887931 \\ \angle FB'E = \arctan(0.2887931) = 16.11^\circ \\ \angle OB'E = 16.11^\circ + 60^\circ = 76.11^\circ \\ \angle OEB' = 180^\circ - 30^\circ - 76.11^\circ = 73.89^\circ \\ B'E = \dfrac{B'F}{\cos 16.11^\circ} = \dfrac{1}{2}\sqrt{\dfrac{2}{3}}\sigma_s \dfrac{1}{\cos 16.11^\circ} = 0.4249352\sigma_s \end{cases} \tag{15}$$

Thus, the locus of the MIF yield criterion is a non-equiangular dodecagon which intersects with the Mises circle. Six points of the dodecagon coincide with the Mises circle, the apex angle is 152.22°; the other six points are outside of the Mises circle, the distance between the points and the circle is $0.0085095\sigma_s$, the apex angle is 147.78°. The side length of the dodecagon is $0.4249352\sigma_s$.

2.3 Plastic work rate per unit volume

It is known that the stress component σ_{ij} satisfies the equation $f(\sigma_{ij}) = 0$, and the strain rate tensor $\dot{\varepsilon}_{ij}$ satisfies the Levy–Mises flow rule [28], written as

$$\dot{\varepsilon}_{ij} = \mathrm{d}\lambda \frac{\partial f}{\partial \sigma_{ij}} \tag{16}$$

When the stress point is on the line $A'E$ described by Eq. (8a), then according to Eq. (16), we can have

$$\dot{\varepsilon}_1 : \dot{\varepsilon}_2 : \dot{\varepsilon}_3 = \mathrm{d}\lambda : -\frac{1 - 2\sqrt{3} + \sqrt{13}}{4}\mathrm{d}\lambda : -\frac{3 + 2\sqrt{3} - \sqrt{13}}{4}\mathrm{d}\lambda \tag{17}$$

Similarly, from Eqs. (8b) and (16), we can have

$$\dot{\varepsilon}_1 : \dot{\varepsilon}_2 : \dot{\varepsilon}_3 = \frac{3 + 2\sqrt{3} - \sqrt{13}}{4}\mathrm{d}\mu : \frac{1 - 2\sqrt{3} + \sqrt{13}}{4}\mathrm{d}\mu : -\mathrm{d}\mu \tag{18}$$

At a corner point, the strain rate components can be obtained by the linear combination of those on the two associated lines [29]. According to this theory, the strain rate at the present point E can be mathematically expressed by

$$\dot{\varepsilon}_i = \mathrm{d}\lambda \frac{\partial f^{\mathrm{MIF}}_{A'E}}{\partial \sigma_i} + \mathrm{d}\mu \frac{\partial f^{\mathrm{MIF}}_{B'E}}{\partial \sigma_i} \tag{19}$$

Thus, the ratio of the strain rate components at the point E can be obtained as

$$\begin{aligned} \dot{\varepsilon}_1 : \dot{\varepsilon}_2 : \dot{\varepsilon}_3 = {} & \left(\mathrm{d}\lambda + \frac{3 + 2\sqrt{3} - \sqrt{13}}{4}\mathrm{d}\mu\right) : \frac{1 - 2\sqrt{3} + \sqrt{13}}{4}(\mathrm{d}\mu - \mathrm{d}\lambda) : \\ & -\left(\frac{3 + 2\sqrt{3} - \sqrt{13}}{4}\mathrm{d}\lambda + \mathrm{d}\mu\right) \end{aligned} \tag{20}$$

If we select $\dot{\varepsilon}_1 = \mathrm{d}\lambda + (3 + 2\sqrt{3} - \sqrt{13})/4\ \mathrm{d}\mu$, then the rest two strain rate components can be expressed as:

$$\dot{\varepsilon}_2 = \frac{1 - 2\sqrt{3} + \sqrt{13}}{4}(\mathrm{d}\mu - \mathrm{d}\lambda);\ \ \dot{\varepsilon}_3 = \left(-\frac{3 + 2\sqrt{3} - \sqrt{13}}{4}\mathrm{d}\lambda - \mathrm{d}\mu\right) \tag{21}$$

Taking notice of $\dot{\varepsilon}_{\max} = \dot{\varepsilon}_1$, $\dot{\varepsilon}_{\min} = \dot{\varepsilon}_3$, we can have

$$\dot{\varepsilon}_{\max} - \dot{\varepsilon}_{\min} = \frac{7 + 2\sqrt{3} - \sqrt{13}}{4}(\mathrm{d}\lambda + \mathrm{d}\mu);\ (\mathrm{d}\lambda + \mathrm{d}\mu) = \frac{4(\dot{\varepsilon}_{\max} - \dot{\varepsilon}_{\min})}{7 + 2\sqrt{3} - \sqrt{13}} \tag{22}$$

It can be noticed that $\sigma_2 = (\sigma_1 + \sigma_3)/2$ at the point E, so we can calculate from Eq. (8) that

$$\sigma_1 - \sigma_3 = \frac{8}{7 + 2\sqrt{3} - \sqrt{13}}\sigma_{\mathrm{s}} \tag{23}$$

The plastic work rate per unit volume (or called the specific plastic work rate) can be calculated as

$$\begin{aligned} D(\dot{\varepsilon}_{ij}) &= \sigma_1\dot{\varepsilon}_1 + \sigma_2\dot{\varepsilon}_2 + \sigma_3\dot{\varepsilon}_3 \\ &= \sigma_1\left(\mathrm{d}\lambda + \frac{3 + 2\sqrt{3} - \sqrt{13}}{4}\mathrm{d}\mu\right) + \frac{1 - 2\sqrt{3} + \sqrt{13}}{4}\sigma_2(\mathrm{d}\mu - \mathrm{d}\lambda) \\ &\quad + \sigma_3\left(-\frac{3 + 2\sqrt{3} - \sqrt{13}}{4}\mathrm{d}\lambda - \mathrm{d}\mu\right) \end{aligned}$$

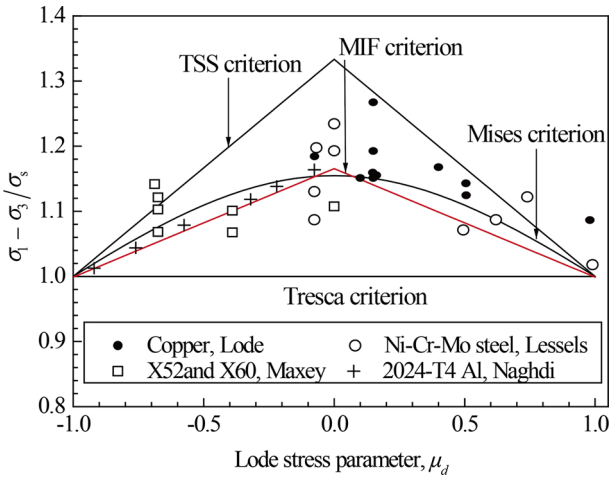

Fig. 5 Comparison of MIF and experimental data

$$
\begin{aligned}
&= \frac{7+2\sqrt{3}-\sqrt{13}}{8}(\sigma_1-\sigma_3)(\mathrm{d}\mu+\mathrm{d}\lambda)\\
&= \frac{7+2\sqrt{3}-\sqrt{13}}{8}\times\frac{8}{7+2\sqrt{3}-\sqrt{13}}\sigma_s\times\frac{4}{7+2\sqrt{3}-\sqrt{13}}(\dot{\varepsilon}_{\max}-\dot{\varepsilon}_{\min})\\
&= \frac{4}{7+2\sqrt{3}-\sqrt{13}}(\dot{\varepsilon}_{\max}-\dot{\varepsilon}_{\min})
\end{aligned}
\tag{24}
$$

2.4 Experimental verification

In order to compare the above-mentioned criteria, the TSS, Mises and the MIF yield criteria can be expressed by the Lode parameters μ_d. As given, the TSS yield criterion can be written as

$$
\frac{\sigma_1-\sigma_3}{\sigma_s}=\begin{cases}\frac{4+\mu_d}{3}, & -1\le\mu_d\le 0\\ \frac{4-\mu_d}{3}, & 0\le\mu_d\le 1\end{cases}
\tag{25}
$$

Similarly, the Mises yield criterion can be expressed as

$$
\frac{\sigma_1-\sigma_3}{\sigma_s}=\frac{2}{\sqrt{3+\mu_d^2}},\quad -1\le\mu_d\le 1
\tag{26}
$$

The MIF yield criterion can be written as

$$
\frac{\sigma_1-\sigma_3}{\sigma_s}=\begin{cases}\frac{8+(1-2\sqrt{3}+\sqrt{13})\mu_d}{7+2\sqrt{3}-\sqrt{13}}, & -1\le\mu_d\le 0\\ \frac{8-(1-2\sqrt{3}+\sqrt{13})\mu_d}{7+2\sqrt{3}-\sqrt{13}}, & 0\le\mu_d\le 1\end{cases}
\tag{27}
$$

According to the above rewritten expressions, the comparison of the Tresca, Mises, TSS, and the MIF yield criteria is illustrated in Fig. 5. The experimental data of copper [30], the Ni-Cr-Mo steel [31], 2024-T4 aluminum [32], and the X52 and X60 pipeline steels [33] are also shown in this figure.

As shown in the figure, the TSS yield criterion gives the upper limit of the experimental data, the Tresca yield criterion gives the lower limit, the result of the MIF yield criterion falls in between the above two criteria. The MIF criterion fits the experimental data very well and has a high approximation degree to the Mises yield criterion. As for the phenomenon that the TSS yield criterion violates various experimental data, which can be attributed to the excessive weight coefficient for the second bigger principal shear stress from its original yield assumption. This shortage has been pointed out by Yu in his subsequent work in Ref. [14].

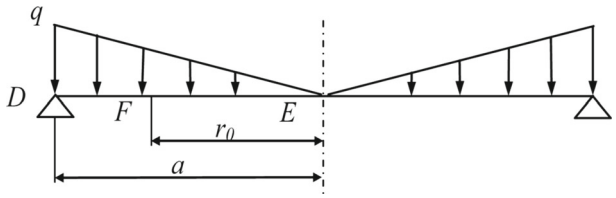

Fig. 6 Simply supported circular plate under linearly distributed load

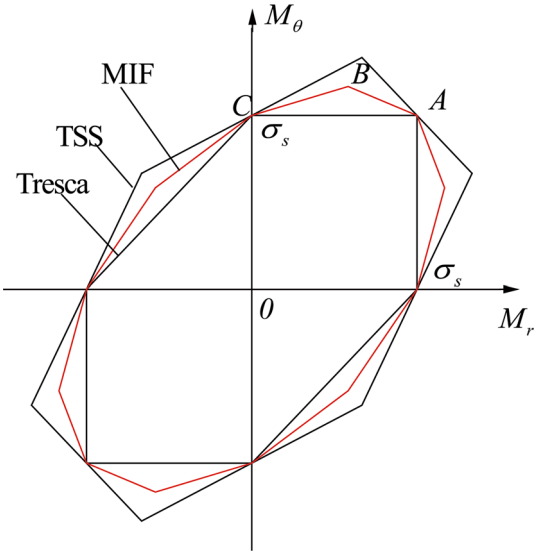

Fig. 7 MIF locus in the plane stress state

3 Analysis of limit load of circular plate by the MIF yield criterion

3.1 Basic equation

A circular plate, with the maximum radius a and thickness h, undergoes a linearly distributed loading q, as shown in Fig. 6.

In the figure, the r is defined as the variable radius in the range of $0 \sim a$. Due to the symmetry, the equilibrium differential equation of the plate can be written as

$$\frac{\mathrm{d}}{\mathrm{d}r}(rM_r) - M_\theta = -\int_0^r rq(r)\mathrm{d}r \tag{28}$$

In the form of generalized stress, the radial bending moment M_r and the tangent bending moment M_θ can be written as [34]

$$M_r = \int_{-\frac{h}{2}}^{\frac{h}{2}} \sigma_r z \mathrm{d}r, \quad M_\theta = \int_{-\frac{h}{2}}^{\frac{h}{2}} \sigma_\theta z \mathrm{d}r \tag{29}$$

In Eq. (29), σ_r is radial normal stress, σ_θ is tangential normal stress, and z is the coordinate which is perpendicular to the circular plate plane.

In the form of generalized stress, the MIF yield criterion in the plane stress state is illustrated in Fig. 7. The points A, B, and C in Fig. 7 correspond to the points E, F, and D in Fig. 6.

Because the deformation of the circular plate belongs to the plane stress problem, the MIF yield criterion in plane stress state can be written as

$$\sigma_\theta - \frac{1-2\sqrt{3}+\sqrt{13}}{4}\sigma_r = \sigma_s,\ \sigma_r \le \frac{\sigma_\theta}{2} \tag{30a}$$

$$\frac{3+2\sqrt{3}-\sqrt{13}}{4}\sigma_\theta + \frac{1-2\sqrt{3}+\sqrt{13}}{4}\sigma_r = \sigma_s,\ \sigma_r \ge \frac{\sigma_\theta}{2} \tag{30b}$$

The equations of AB and BC are derived from Eq. (30), written as

$$\frac{3+2\sqrt{3}-\sqrt{13}}{4}M_\theta + \frac{1-2\sqrt{3}+\sqrt{13}}{4}M_r = M_p \tag{31a}$$

$$M_\theta - \frac{1-2\sqrt{3}+\sqrt{13}}{4}M_r = M_p \tag{31b}$$

where the plastic limit bending moment can be calculated by $M_p = \sigma_s h^2/4$.

3.2 Calculation of the limit load

The calculating diagram of the limit load is shown in Fig. 6, and the q is defined as the linearly distributed load. By assuming that the bending moment at the point F is equal to that at the point B in Fig. 6, and substituting Eqs. (31a) and (31b) into Eq. (28), then the equilibrium equations of EF and FD can be written as

EF:

$$r \cdot \frac{dM_r}{d_r} = \frac{4}{3+2\sqrt{3}-\sqrt{13}}M_p - \frac{4}{3+2\sqrt{3}-\sqrt{13}}M_r - \frac{qr^3}{3a} \tag{32a}$$

FD:

$$r \cdot \frac{dM_r}{d_r} = M_p - \frac{3+2\sqrt{3}-\sqrt{13}}{4}M_r - \frac{qr^3}{3a} \tag{32b}$$

Equation (32a) is a first-order non-homogeneous linear differential equation. After calculation, the corresponding homogeneous equation and its general solution can be solved as

$$\frac{d(M_p - M_r)}{(M_p - M_r)} = -\frac{4}{3+2\sqrt{3}-\sqrt{13}}\frac{\mathrm{d}r}{r} \tag{33a}$$

$$M_r = M_p - Cr^{\frac{-4}{3+2\sqrt{3}-\sqrt{13}}} \tag{33b}$$

According to the constant variation method [35], the general stress of EF can be calculated as

$$\begin{cases} M_r = C_1 r^{\frac{-4}{3+2\sqrt{3}-\sqrt{13}}} + M_p - \dfrac{3+2\sqrt{3}-\sqrt{13}}{39+18\sqrt{3}-9\sqrt{13}}\dfrac{qr^3}{a},\ C_1 = -\dfrac{3+2\sqrt{3}-\sqrt{13}}{4}C_0 \\ M_\theta = -\dfrac{1-2\sqrt{3}+\sqrt{13}}{3+2\sqrt{3}-\sqrt{13}}C_1 r^{\frac{-4}{3+2\sqrt{3}-\sqrt{13}}} + M_p + \dfrac{1-2\sqrt{3}+\sqrt{13}}{39+18\sqrt{3}-9\sqrt{13}}\dfrac{qr^3}{a} \end{cases} \tag{34a}$$

Similarly, the general stress of FD can be calculated as

$$\begin{cases} M_r = C_2 r^{-\frac{3+2\sqrt{3}-\sqrt{13}}{4}} + \dfrac{4}{3+2\sqrt{3}-\sqrt{13}}M_p - \dfrac{4}{45+6\sqrt{3}-3\sqrt{13}}\dfrac{qr^3}{a} \\ M_\theta = -\dfrac{1-2\sqrt{3}+\sqrt{13}}{4}C_2 r^{-\frac{3+2\sqrt{3}-\sqrt{13}}{4}} + \dfrac{4}{3+2\sqrt{3}-\sqrt{13}}M_p - \dfrac{1-2\sqrt{3}+\sqrt{13}}{45+6\sqrt{3}-3\sqrt{13}}\dfrac{qr^3}{a} \end{cases} \tag{34b}$$

In Eq. (34), the boundary condition at the center of the plate is $M_r|_{r=0} = M_\theta|_{r=0} = M_p$ and at the edge is $M_r|_{r=a} = 0$. Then, C_1 and C_2 can be solved as

$$C_1 = 0,\ C_2 = \left[-\frac{4}{3+2\sqrt{3}-\sqrt{13}}M_p + \frac{4}{45+6\sqrt{3}-3\sqrt{13}}\frac{qr^2}{a}\right] \cdot a^{\frac{3+2\sqrt{3}-\sqrt{13}}{4}} \tag{35}$$

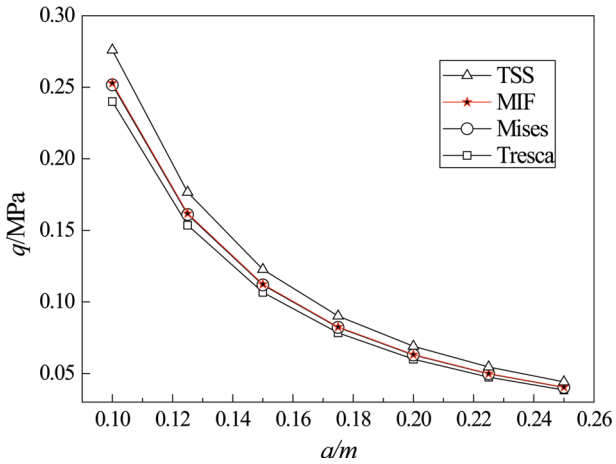

Fig. 8 Effect of different criteria on the limit load

It can be derived from Eqs. (31a) and (31b) that $2M_r|_{r=0} = M_\theta|_{r=0}$ at the point B. By applying this condition into Eqs. (34a) or (34b) and taking notice of $C_1 = 0$, then the limit load can be calculated as

$$q^{\mathrm{MIF}} = \frac{39 + 18\sqrt{3} - 9\sqrt{13}}{7 + 2\sqrt{3} - \sqrt{13}} \cdot \frac{aM_\mathrm{p}}{r_0^3} \tag{36}$$

Substituting q_I^{MIF} and C_2 into Eq. (34b) and taking notice of $2M_r|_{r=0} = M_\theta|_{r=0}$, then the equation for the radius r_0 (i.e., the radius at point B in Fig. 6) where the tangential stress reaches the maximum value, can be calculated as

$$\left[0.8464\left(\frac{a}{r_0}\right)^3 - 2.3993\right] \cdot \left(\frac{a}{r_0}\right)^{\frac{3+2\sqrt{3}-\sqrt{13}}{4}} + 0.5529 = 0 \tag{37}$$

It can be seen from Eq. (37) that the solution only relies on the value of a/r_0. After calculation, the value of r_0 is $0.7577a$. Thus, the limit load can be solved as

$$q^{\mathrm{MIF}} = \frac{12.6436M_\mathrm{p}}{a^2} \tag{38}$$

3.3 Parametric analysis and FEM verification

For this problem, the limit load has ever been obtained based on the Tresca yield criterion directly and has also been numerically simulated by the Mises yield criterion and fitted into a equation [36]. The analytical Tresca solution and the Mises fitted expression can be shown as follows:

$$q^{\mathrm{Tresca}} = \frac{12M_\mathrm{p}}{a^2},\ q^{\mathrm{Mises}} = \frac{12.5829M_\mathrm{p}}{a^2} \tag{39}$$

The expression of the limit load based on the TSS yield criterion, denoted by q^{TSS}, carried out by Yu et al. [37], can be written as

$$q^{\mathrm{TSS}} = \frac{5aM_\mathrm{p}}{r_0^2},\ a \approx 1.3889r_0 \tag{40}$$

There exists a plate with thickness $h = 1$ mm. The yield stress of this plate is $\sigma_\mathrm{s} = 800$ MPa. The effect of different yield criteria on the limit load is shown in Fig. 8.

It can be observed that the upper bound of the limit load is predicted by the TSS yield criterion, and the lower bound of the limit load is predicted by the Tresca yield criterion. The predicted result based on the MIF

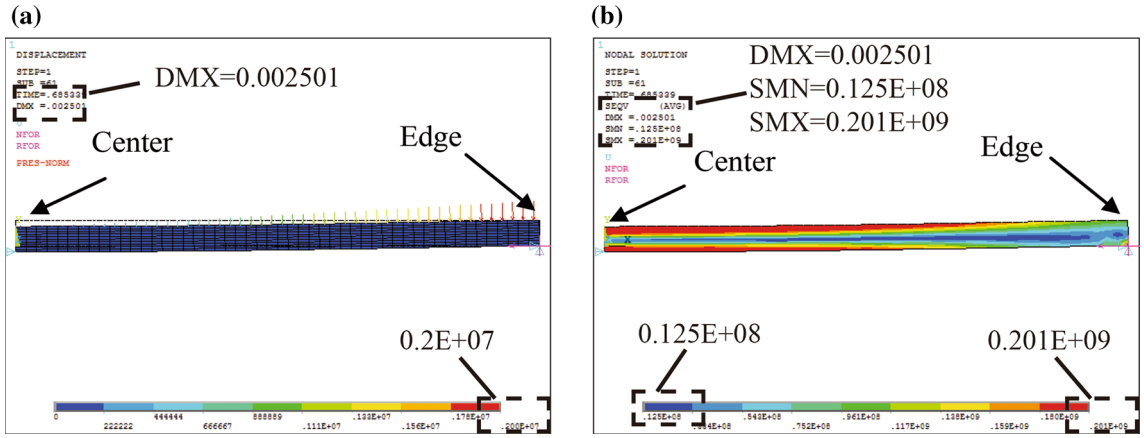

Fig. 9 **a** Deformation shape; **b** effective stress contour

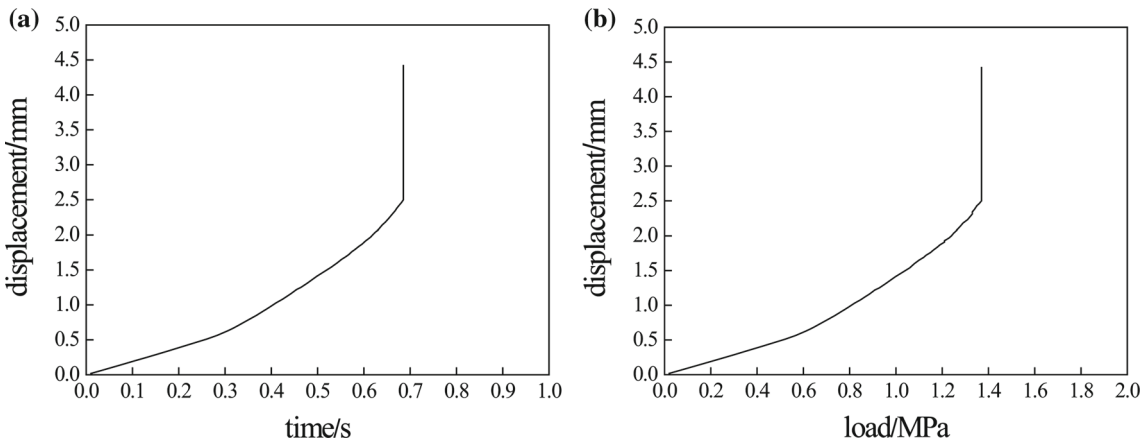

Fig. 10 Time–displacement (**a**) and load–displacement (**b**) curves at dangerous point

yield criterion is between those by the two criteria. The present result has a high approximation degree to that of the Mises yield criterion.

The simply supported circular plate under a linear distributed load can also be modeled and analyzed using the finite element method, which is carried out here to further check the correctness of the proposed yield criterion. In the ANSYS, the Mises yield criterion implemented in the software is still used and the simply supported circular plate is numerically simulated with the Plane 182 element. It can be assumed that the material model is elastoplastic material, and the modulus of elasticity E is 200 GPa, yield strength σ_s is 200 MPa, strain-hardening modulus E_r is 0 MPa, Poisson's ratio υ is 0.499, radius of the circular plate a is 0.2 m, plate thickness $2h$ is 10 mm. It should be noted that the metal-hardening effect has not been considered in this simulation so as to keep consistent with the theoretical calculation in terms of a fixed σ_s. This becomes the weakness of the present study, which will be modified in our further work.

After the simulation, the deformation shape and the effective stress contour of the circle plate under the linear load can be obtained, as shown in Fig. 9.

It can be seen from Fig. 9 that the deflection at the center of the circular plate is the largest, and the closer the circular plate approaches to the center, the larger the equivalent stress is. The center of the circular plate will enter the yield state firstly and then the plastic zone will expand outward. At the center of the circular plate, the time–displacement curve and load–displacement curve at dangerous point are shown in Fig. 10a, b.

From Fig. 10, it can be seen that there is a corresponding relationship between the time and load. The load is diverged when the time step is 0.68534 s, and the applied load is 2 MPa. So, the simulated value of the limit load can be solved as $2\,\text{MPa} \times 0.68543 = 1.37068\,\text{MPa}$.

The relative error between the theoretical solution based on the MIF yield criterion and the numerical solution based on the Mises yield criterion is -12.85%, and the deviation is acceptable in engineering application($<15\%$), which verifies the correctness of the analytical solution.

4 Forging analysis of a rectangular bar by the MIF criterion

4.1 Procedure description

Under the condition of $0.6 \sim 0.5 < l/h < 6 \sim 4$, a rectangular bar is forged and pressed through a rough hammer, which belongs to plane deformation problem. As shown in Figs. 11 and 12, the billet grid on cross section has a parabolic shape. The adhesive zone completely covers the contact surface, and the broadside is deformed as a single bulged shape. Thus, the contact friction stress can be written as

$$\tau_f = \frac{m\sigma_s}{\sqrt{3}} \tag{41a}$$

The value of m can be calculated by the Тарновский formula [37]:

$$m = f + \frac{1}{8}\frac{l}{h}(1-f)\sqrt{f} \tag{41b}$$

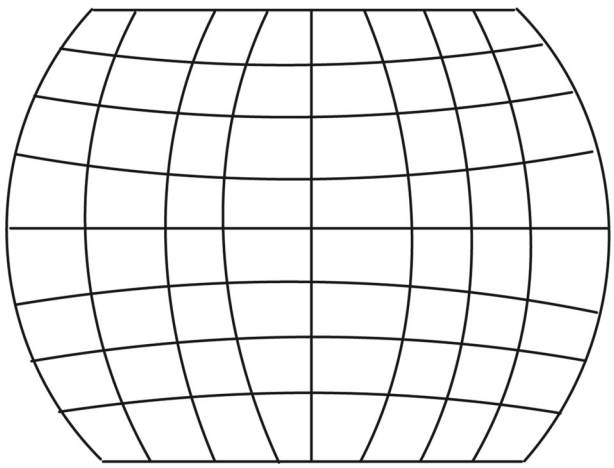

Fig. 11 Grid of the rectangular part on the cross section after compression

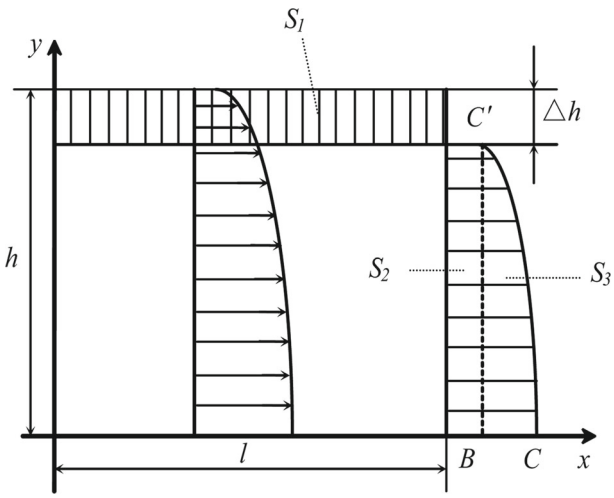

Fig. 12 Coordinate system and displacement field

where f is the sliding friction coefficient.

4.2 Displacement field

As shown in Fig. 11, because of the symmetry in the deformation zone, only one-fourth of the part is analyzed. Therefore, the displacement field can be set as

$$u_x = a_0 x + ax\left(1-\frac{3y^2}{h^2}\right)\left(1-\frac{1}{3}\frac{x^2}{l^2}\right),\ u_y = -\left[a_0 y + ay\left(1-\frac{y^2}{h^2}\right)\left(1-\frac{x^2}{l^2}\right)\right],\ u_z = 0 \tag{42}$$

Because of the plastic deformation caused by the forging process, there is a nonlinear relationship between strain and displacement. In this case, the strain field can be determined by the Cauchy's equation [27] which describes the incremental relationship between displacement component and coordinate axis. Thus, the strain field based on the above displacement field can be derived as

$$\begin{cases} \varepsilon_x = \frac{\partial u_x}{\partial x} = a_0 + a\left(1-\frac{3y^2}{h^2}\right)\left(1-\frac{1}{3}\frac{x^2}{l^2}\right) \\ \varepsilon_y = \frac{\partial u_y}{\partial y} = -a_0 - a\left(1-\frac{3y^2}{h^2}\right)\left(1-\frac{1}{3}\frac{x^2}{l^2}\right) \\ \varepsilon_z = \frac{\partial u_z}{\partial z} = 0 \\ \varepsilon_{xy} = \frac{1}{2}\left(\frac{\partial u_x}{\partial y}+\frac{\partial u_y}{\partial x}\right) = -a\frac{3xy}{h^2}\left(1-\frac{1}{3}\frac{x^2}{l^2}\right) + a\frac{xy}{l^2}\left(1-\frac{3y^2}{h^2}\right) \\ \varepsilon_{yx} = \frac{1}{2}\left(\frac{\partial u_y}{\partial x}+\frac{\partial u_x}{\partial y}\right) = -a\frac{3xy}{h^2}\left(1-\frac{1}{3}\frac{x^2}{l^2}\right) + a\frac{xy}{l^2}\left(1-\frac{3y^2}{h^2}\right) \\ \varepsilon_{xz} = \varepsilon_{zx} = \varepsilon_{yz} = \varepsilon_{zy} = \varepsilon_z = 0 \end{cases} \tag{43}$$

where a is the geometrical deformation coefficient.

According to the volume-constancy condition and the mean value theorem, we can obtain

$$\Delta h \cdot l = \int_0^h u_x|_{x=l}\,\mathrm{d}y,\ a_0 = \frac{\Delta h}{h} = \varepsilon \tag{44}$$

It can be noticed that $\varepsilon_x = \varepsilon_y = \varepsilon$ and the other strains are zero. Thus, the axes in Eq. (42) are principal axes. Then it produces

$$\varepsilon_{\max} = a_0 + a\left(1-\frac{3y^2}{h^2}\right)\left(1-\frac{1}{3}\frac{x^2}{l^2}\right),\ \varepsilon_{\min} = -\left[a_0 + a\left(1-3\frac{y^2}{h^2}\right)\left(1-\frac{x^2}{l^2}\right)\right] \tag{45}$$

4.3 Theoretical analysis and verification

4.3.1 Total energy functional

By referencing Eq. (24), the internal plastic deformation work can be written as

$$\begin{aligned} \phi_1 &= \int_0^l\int_0^h D(\varepsilon_{ik})\mathrm{d}x\mathrm{d}y = \frac{4}{7+2\sqrt{3}-\sqrt{13}}\sigma_s\int_0^l\int_0^h(\varepsilon_{\max}-\varepsilon_{\min})\mathrm{d}x\mathrm{d}y \\ &= \frac{8}{7+2\sqrt{3}-\sqrt{13}}\sigma_s\int_0^l\int_0^h\left[a_0 + a\left(1-3\frac{y^2}{h^2}\right)\left(1-\frac{x^2}{l^2}\right)\right]\mathrm{d}x\mathrm{d}y \\ &= \frac{8}{7+2\sqrt{3}-\sqrt{13}}\sigma_s a_0 lh \end{aligned} \tag{46}$$

According to Eq. (42), the friction work on the contact surface can be written as

$$\phi_2 = \frac{m\sigma_s}{\sqrt{3}}\int_0^l u_x|_{y=h}\mathrm{d}x = \frac{m\sigma_s l^2}{\sqrt{3}}\left(\frac{a_0}{2}-\frac{5}{6}a\right) \tag{47}$$

Summation of Eqs. (46) and (47) yields

$$\phi = \frac{8}{7+2\sqrt{3}-\sqrt{13}}\sigma_s a_0 lh + \frac{m\sigma_s l^2}{\sqrt{3}}\left(\frac{a_0}{2}-\frac{5a}{6}\right) = \frac{8}{7+2\sqrt{3}-\sqrt{13}}\sigma_s \varepsilon lh + \frac{m\sigma_s l^2}{\sqrt{3}}\left(\frac{\varepsilon}{2}-\frac{5a}{6}\right) \quad (48)$$

From the balance principle of the internal work and the external work and taking notice of $\bar{p} = P/l \times 1$, $\varepsilon = a_0 = \Delta h/h$, $K = 2k = 2\sigma_s/\sqrt{3}$, then the stress effective factor can be calculated as

$$n_\sigma = \frac{\bar{p}}{K} = 1.0095 + \frac{ml}{4h} - \frac{5a}{12\varepsilon}\frac{ml}{h} \quad (49)$$

4.3.2 Determination of the geometrical coefficient a

From Eq. (42) and Fig. 12, the displacement of C'in the x direction can be written as

$$u_x|_{x=l,y=h} = a_0 l - \frac{4}{3}al = \frac{\Delta h}{h}l - \frac{4}{3}al \quad (50)$$

Similarly, the displacement of C in the x direction can be written as

$$u_x|_{x=l,y=0} = a_0 l + \frac{2}{3}al = \frac{\Delta h}{h}l + \frac{2}{3}al \quad (51)$$

The area of S_3 can be calculated by the area of S_1 minus the area of S_2. Substituting Eq. (51) into the following equation, it produces

$$S_3 = \frac{2b}{3}h_1 = l\Delta h - u_{x|x=l,y=h}h_1 = l\Delta h - \left(\frac{\Delta h}{h}l - \frac{4}{3}al\right)h_1 \quad (52)$$

Solving Eq. (52), then one can determine that

$$a = \frac{b}{2l} - 0.75\left(\frac{\Delta h}{h_1} - \varepsilon\right) \quad (53)$$

where $b = OC - OB = l_m - l_s$, depending on the actual measurement.

4.3.3 Experiment verification

A lead workpiece was compressed at the speed of 25 mm/min on a press machine. The size of the workpiece is $H_0 = 2h_0 = 40$ mm, $L_0 = 2l_0 = 38$ mm, $B = 58$ mm. The material coefficient f is 0.5 measured by a ring upsetting experiment [37]. After compressing, the size of the workpiece is $H_1 = 2h_1 = 36$ mm, $L_{mid} = 2l_{mid}$ is 43 mm, $L_{surface} = 2l_{surface}$ is 40 mm, the measured forging force is 57.6 kN.

For theoretical calculation, we can get $b = l_{mid} - l_{surface} = 1.15$ mm, $\varepsilon = \Delta h/h_0 = 0.1$, $t = \Delta h/v = 4.8$ s, $\dot{\varepsilon} = \varepsilon/t = 0.0208\ s^{-1}$.

Because of the volume-constancy condition, it can be obtained that $2 \times 20 \times 19 = 2 \times 18l_1$, then l_1 is 21.111 mm. Thus, l/h can be obtained as

$$\frac{l}{h} = \frac{(l_0+l_1)/2}{(h_0+h_1)/2} = 1.056 \quad (54)$$

Substituting the above parameters into Eqs. (52) and (41) , it produces

$$a = \frac{1.5}{2\times 19} - 0.75 \times \left(\frac{2}{18} - 0.1\right) = 0.031 \quad (55)$$

$$m = 0.5 - 0.125 \times 1.056 \times 0.5 \times \sqrt{0.5} = 0.547 \quad (56)$$

Substituting $\varepsilon = 0.1$, $\bar{l}/\bar{h} = 1.056$, $a = 0.031$, $m = 0.547$ into Eq. (48), it produces

$$n_\sigma = \frac{\bar{p}}{K} = 1.0797 \quad (57)$$

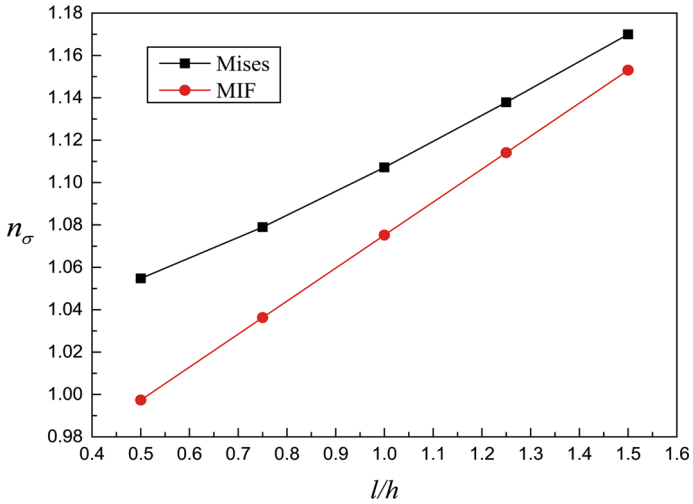

Fig. 13 Comparison of the stress factor of the MIF and the Mises yield criteria

According to ε and $\dot{\varepsilon}$, the value of σ_s can be determined as 20.15 MPa [38], then the total deformation force can be calculated as

$$P = 1.155\sigma_s \cdot n_\sigma \cdot L \cdot B = 58.297\,\text{kN} \tag{58}$$

When compared with the measured value, the relative error of the above result is

$$\Delta_1 = \frac{58.297 - 57.6}{57.6} \times 100\% = 1.21\% \tag{59}$$

4.4 Comparison with Тарновский's result

For this problem, Тарновский has ever proposed the following results based on the Mises yield criterion [39]:

$$\frac{a}{\varepsilon} = \frac{0.4167m\frac{l}{h}}{0.213 + 0.648\frac{l^2}{h^2} + 0.026\frac{h^2}{l^2}} \tag{60}$$

$$n_\sigma = \left[1 + \left(\frac{a}{\varepsilon}\right)^2 \left(0.213 + 0.648\frac{l^2}{h^2} + 0.026\frac{h^2}{l^2}\right)\right]^{\frac{1}{2}} + m\frac{l}{h}\left(0.25 - 0.416\frac{a}{\varepsilon}\right) \tag{61}$$

The Shwarz inequality has been used for amplification for obtaining Eq. (61). Thus, the result is a numerical solution.

Substituting $l/h = 1.056$ and $m = 0.547$ into above equation, it produces

$$\frac{a}{\varepsilon} = 0.251\,,\ n_\sigma = 1.1139 \tag{62}$$

Thus, the total pressure P can be calculated as $P = 1.155(\sigma_s \cdot n_\sigma \cdot L \cdot B) = 60.14\,\text{kN}$. When compared with the measured value, the relative error between them is

$$\Delta_2 = \frac{60.14 - 57.6}{57.6} \times 100\% = 4.41\% \tag{63}$$

It can be obtained from Δ_1 and Δ_2 that the results based on two criteria are both bigger than actual one, but the result of the MIF criterion is more precise. What is more, the MIF criterion is a linear yield criterion, and its specific plastic work rate is also linear, which creates the condition of obtaining the analytical solution, i.e., Eq. (49).

The stress effective factor n_σ calculated by two criteria can be obtained and is shown in Fig. 13.

It can be observed that the results of the MIF are slightly lower. The analytical solution, Eq. (49), is much more simple than Тарновский's result, Eq. (61). Additionally, it can be obtained from Fig. 13 that n_σ increases with increasing l/h.

5 Conclusions

(1) By considering the difference of the intermediate principle stresses of the Tresca, Mises, and TSS yield criteria, a new yield criterion shown as a dodecagon is proposed through the method of parabolic interpolation and mathematical averaging. The locus of the criterion is an equilateral and non-equiangular dodecagon. The apex angles of the yield locus are 152.22° and 147.78°, and the length of the side of the dodecagon is $0.4249352\sigma_s$.

(2) The proposed yield criterion coincides well with experimental data and varies linearly with the Lode parameter. The yield criterion lies in between the Tresca and TSS yield criteria, and approaches well to the Mises yield criterion.

(3) The limit load of the simply supported circular plate calculated by this criterion is a function of a and h. The load reaches the limit when $r_0 = 0.7577a$, and the relative error between the theoretical solution and the numerical solution is 12.85%.

(4) The specific work rate $D(\dot{\varepsilon}_{ij})$ is derived as $4/(7 + 2\sqrt{3} - \sqrt{13})\sigma_s(\dot{\varepsilon}_{\max} - \dot{\varepsilon}_{\min})$. It can be used in the analysis of the forging force of a rectangular bar, and the analytical solution can be obtained. The result indicates that the stress state coefficient increases with the increase of l/h. The predicted value calculated by the MIF criterion is very close to the actual measurement.

Acknowledgements This research was supported by the National Natural Science Foundation of China (Grant Nos. U1960105, 51504156), the Outstanding Youth Fund of Jiangsu Province (Grant No. BK20180095), the Prospective Applied Research from the Technological Innovation Project of Key Industry of Suzhou (Grant No. SYG201806), as well as supported by State Key Laboratory of Materials Processing and Die & Mould Technology, Huazhong University of Science and Technology (Grant No. P2019-015). The authors also wish to acknowledge valuable suggestions from reviewers.

Compliance with ethical standards

Conflict of interest The authors declare that they have no conflict of interest.

References

1. Coulomb, C.A.: Essai sur une application des règles de maximis et minimis à quelques problèmes de statique relatifs à l'architecture. Mem. Divers. Savants **7**, 343–82 (1776)
2. Tresca, H.: Memoir on the flow of solid bodies under strong pressure. Comptesrendus de l'Académie des Sciences **59**, 754–758 (1864)
3. Saint-Venant, B.: Memoire sur I'etablissement des Equations Differentielles des Mouvements Interieurs Operes Dans Les Corps Solides Ductiles au Dela des Limites ou I'elasticite Pourrait Les Ramener a Leur Premier etat. C. R. Acad. Sci. Paris **70**, 473–480 (1870)
4. Levy, M.: Memoire Sur Les Equations Generales des Mouvements Interieurs des Corps Solides Ductiles au Dela Limits ou 1'Elasticite Pourrait Les Rammener a LeurPpremier etat. C. R. Acad. Sci. Paris **70**, 1323–1325 (1870)
5. Mises, R.V.: Mechanik der festen Körper im plastisch-deformablen Zustand. Nachr. Ges. Wiss. Gött. Math. Phys. Kl. **1913**(4), 582–592 (1913)
6. Huber, M.T.: Przyczynek do podstaw wytoryalsci. Czas. Tech. **22**, 81–82 (1904)
7. Hencky, H.: Zur Theorie plastischer Deformationen und der hierdurch im Material hervorgerufenen Nachspannungen. ZAMM J. Appl. Math. Mech. Zeit. Angew. Math. Mech. **4**(4), 323–334 (1924)
8. Mises, R.V.: Mechanik der plastischen Formänderung von Kristallen. ZAMM J. Appl. Math. Mech. **8**(3), 161–185 (1928)
9. Hill, R.: A Theory of the Yielding and Plastic Flow of Anisotropic Metals. Proc. R. Soc. Lond. Ser. A Math. Phys. Sci. **193**(1033), 281–297 (1948)
10. Prager, W.: Introduction to mechanics of continua. Numer. Methods Algorithms **29**(2), 385–403 (2005)
11. Drucker, D.C.: A more fundamental approach to plastic stress–strain relations. In: Proceedings of the 1st US National Congress for Applied Mechanics, pp. 487–491. ASME (1951)
12. Yu, M.H.: Advances in strength theories for materials under complex stress state in the 20th century. Appl. Mech. Rev. **55**(3), 169–218 (2002)
13. Yu, M.H.: Twin shear stress yield criterion. Int. J. Mech. Sci. **25**(1), 71–74 (1983)
14. Yu, M.H.: Twin Shear Theory and Its Applications. Academic Press, Beijing (1998). **(in Chinese)**

15. Yu, M.H.: Unified Strength Theory and Its Applications. Springer, Berlin (2004)
16. Hu, X.R., Yu, M.H.: Study on the three shear stress criterion for materials. Eng. Mech. **23**(4), 6–11 (2006). **(in Chinese)**
17. Zhu, X.K., Leis, B.N.: Average shear stress yield criterion and its application to plastic collapse analysis of pipelines. Int. J. Press. Vessels Pip. **83**(9), 663–671 (2006)
18. Zhu, X.K., Leis, B.N.: Evaluation of burst pressure prediction models for line pipes. Int. J. Press. Vessels Pip. **89**, 85–97 (2012)
19. Barsanescu, P.D., Comanici, A.M.: von Mises hypothesis revised. Acta Mech. **228**(2), 433–446 (2017)
20. Gu, J., Chen, P.: A failure criterion for homogeneous and isotropic materials distinguishing the different effects of hydrostatic tension and compression. Eur. J. Mech. A/Solids **70**, 15–22 (2018)
21. Pei, J., Einstein, H.H., Whittle, A.J.: The normal stress space and its application to constructing a new failure criterion for cross-anisotropic geomaterials. Int. J. Rock Mech. Min. Sci. **106**, 364–373 (2018)
22. Böhlke, T., Bertram, A., Krempl, E.: Modeling of deformation induced anisotropy in free-end torsion. Int. J. Plast. **19**(11), 1867–1884 (2003)
23. Langer, J.S., Bouchbinder, E., Lookman, T.: Thermodynamic theory of dislocation-mediated plasticity. Acta Mater. **58**(10), 3718–3732 (2010)
24. Langer, J.S.: Thermal effects in dislocation theory. Phys. Rev. E **94**(6), 063004 (2016)
25. Le, K.C., Tran, T.M., Langer, J.S.: Thermodynamic dislocation theory of adiabatic shear banding in steel. Scr. Mater. **149**, 62–65 (2017)
26. Le, K.C.: Thermodynamic dislocation theory for non-uniform plastic deformations. J. Mech. Phys. Solids **111**, 157–169 (2018)
27. Avitzur, B.: Metal Forming: The Application of Limit Analysis. Marcel Dekker Inc., New York (1980)
28. Le May, I.: Principles of Mechanical Metallurgy. Elsevier, New York (1983)
29. Zhou, Y.C.: Solid Mechanics of Materials. Science Press, Beijing (2005). **(in Chinese)**
30. Lode, W.: Versuche über den Einfluß der mittleren Hauptspannung auf das Fließen der Metalle Eisen, Kupfer und Nickel. Zeitschrift für Physik A Hadrons and Nuclei **36**(11), 913–939 (1926)
31. Lessells, J.M., MacGregor, C.W.: Combined stress experiments on a nickel–chrome–molybdenum steel. J. Frankl. Inst. **230**(2), 163–181 (1940)
32. Naghdi, P.M., Essenburg Jr., F., Koff, W.: An experimental study of initial and subsequent yield surfaces in plasticity. Appl. Mech. **25**, 201–9 (1958)
33. Maxey, W.A.: Measurement of yield strength in the mill expander. In: Proceedings of the Fifth Symposium on Line Pipe Research, pp. 20–22 (1974)
34. Liu, F.L., Meng, F.X., Peng, Y.: Limit analysis of simply supported circular plate under linear distributed load with Mises criterion. Eng. Mech. (Supplement) **33**, 325–327 (2002)
35. Zhang, S.H., Gao, C.R., Zhao, D.W., et al.: limit load analysis of simply supported circular plate under linearly distributed load with GM criterion. Chin. J. Comput. Mech. **2**, 021 (2013)
36. Wang, T.B., Yu, M.H.: Unified plastic solution to circular plate with considering the effect of strength-difference. Chin. J. Appl. Mech. **20**(1), 144–148 (2003)
37. Zhao, D.W.: The Principle and Application of Linear Forming Energy Rate Integral. Metallurgical Industry Press, Beijing (2012). **(in Chinese)**
38. Xu, Y.S., Xu, H.L., Huang, X.L.: On measuring friction factor by means of upsetting ring. J. Taiyuan Inst. Mach. **11**(4), 53–61 (1990). **(in Chinese)**
39. Zhao, Z.Y., Wang, G.D.: Modern Plastic Machining Mechanics. Northeastern University of Technology Press, Shenyang (1986). **(in Chinese)**